JOURNAL OF AGRICULTURAL AND FOOD CHEMISTRY
ARTICLE

J. Agric. Food Chem. 2010, 58, 3681–3688 3681
DOI:10.1021/jf904385c

Bioactivity of Chemically Transformed Humic Matter from Vermicompost on Plant Root Growth

Leonardo Barros Dobbss,[†] Luciano Pasqualoto Canellas,*[,†] Fábio Lopes Olivares,[†] Natália Oliveira Aguiar,[†] Lázaro Eustáquio Pereira Peres,[‡] Mariana Azevedo,[‡] Riccardo Spaccini,[§,#] Alessandro Piccolo,[§,#] and Arnoldo R. Façanha[†]

[†]Núcleo de Desenvolvimento de Insumos Biológicos para Agricultura (NUDIBA), Universidade Estadual do Norte Fluminense Darcy Ribeiro (UENF), Av. Alberto Lamego 2000, Campos dos Goytacazes 28013-602, Rio de Janeiro, Brazil, [‡]Departamento de Ciências Biológicas, Escola Superior de Agricultura "Luiz de Queiroz" (ESALQ), Universidade de São Paulo (USP), Av. Padua Dias 11, CP. 09, 13418-900 Piracicaba, Brazil, [§]Dipartimento di Scienze del Suolo, della Pianta, dell'Ambiente e delle Produzioni Animali (R.S., A.P.), and [#]Centro Interdepartamentali per la Spectroscopia della Rizonancia Magnetica Nucleare (CERMANU), Università di Napoli Federico II, Via Università 100, 80055 Portici, Italy

Chemical reactions (hydrolysis, oxidation, reduction, methylation, alkyl compounds detachment) were applied to modify the structure of humic substances (HS) isolated from vermicompost. Structural and conformational changes of these humic derivatives were assessed by elemental analyses, size exclusion chromatography (HPSEC), solid-state nuclear magnetic resonance (^{13}C CPMAS-NMR), and diffusion ordered spectroscopy (DOSY-NMR), whereas their bioactivity was evaluated by changes in root architecture and proton pump activation of tomato and maize. All humic derivatives exhibited a large bioactivity compared to original HS, both $KMnO_4$-oxidized and methylated materials being the most effective. Whereas no general relationship was found between bioactivity and humic molecular sizes, the hydrophobicity index was significanty related with proton pump stimulation. It is suggested that the hydrophobic domain can preserve bioactive molecules such as auxins in the humic matter. In contact with root-exuded organic acids the hydrophobic weak forces could be disrupted, releasing bioactive compounds from humic aggregates. These findings were further supported by the fact that HS and all derivatives used in this study activated the auxin synthetic reporter DR5::GUS.

KEYWORDS: Structural−activity relationship; size exclusion chromatography; NMR spectroscopy; chemical modification; plant biostimulation

INTRODUCTION

The application of products derived from humic substances (HS) at low concentration on crop plants and their potential to act as plant growth promoters have been creating increased interest among farmers. However, there is little information about the mechanisms by which HS influence biological activities in plants. The intrinsic complexity of HS means that the relationships between structure and activity follow a nonlinear trend. Understanding it became a central task in enhancing the efficient use and development of new generations of organic inputs based on humic technology. Evidence of the physiological mechanism through which HS exert their effects may depend on hormones and, in particular, on the presence of auxin or auxin-like components in their structure (*1*). It would be expected that low molecular weight HS can access more easily cell receptors on membranes. However, it was previously verified that a wide range of molecular weight distribution of humic fractions, obtained by size exclusion chromatography, induces lateral root emergence and induces plasma membrane (PM) H^+-ATPase activity (*2*). A significant relationship between the hydrophobic character of humic acids isolated from different soils and enhanced PM H^+-ATPase expression in maize seedlings has been reported (*3*, *4*). The increase in activity of PM H^+-ATPase is in line with the acid growth mechanism (*5*). It was previously postulated that hydrophobic humic components derived from plant degradation and microbial activity are able to randomly incorporate more polar molecules and hence protect them against degradation (*6*). The process of molecular trapping into humic hydrophobic domains suggests that the more hydrophobic the humic acids (HA), the larger the potential hydrophobic incorporation of bioactive molecules, whereas the larger the chemical diversity of such bioactive molecules, the more diverse their bioactivity.

Chemical modification of humic substances has been widely used as a tool to understand their chemical structure (*7*−*10*). Studies of chemical transformation of HS followed by biomonitoring can provide new insights on humus bioactivity.

The aim of this study was to evaluate the influence of chemical modifications of humic structure on root stimulation. The HS were evaluated by elemental composition, HPSEC, CP-MAS ^{13}C

*Corresponding author (telephone +55 22 27397301; e-mail canellas@uenf.br).

Published on Web 02/25/2010

NMR, and DOSY ^{1}H NMR spectroscopies, and their bioactivities were monitored by following the morphological and biochemical traits of *Arabidopsis* (*Arabidopsis thaliana* Heynh), tomato (*Solanum lycopersicum* L.), and maize (*Zea mays* L.).

MATERIALS AND METHODS

Vermicompost Production. A vermicompost was obtained from a mixture of plant residues of guinea grass (*Panicum maximun* Jacq.) and cattle manure 5:1 (v/v). The organic residues were mixed, and earthworms (*Eisenia fetida* Sav.) were added at a ratio of 5 kg/m^3 of organic residue. The organic matter composition of the resulting vermicompost was pH 6.5, 134 g/kg organic carbon, 13.3 g/kg nitrogen, 10:1 C/N ratio, and 16.4 g/kg HA.

Extraction and Purification of HS. HS from vermicompost were extracted using 0.5 M NaOH. After 24 h under N_2 atmosphere, the suspension was centrifuged and the insoluble residue separated. The supernatant pH was then adjusted to pH 3 with 6 M HCl, the resulting solution passed through a XAD-8 column, and the adsorbed material eluted out with 0.1 M NaOH. The eluted solution was adjusted to pH 7 with 1 M HCl and freeze-dried. The HS were redissolved in a reduced volume of distilled water and dialyzed (14 kDa MW cutoff) against deionized water. After dialysis, the HS were freeze-dried again before being chemically derivatized.

Humic Derivatization. *Acidic Oxidation with $KMnO_4$ (D1).* The oxidation reaction was carried out in 20 mL of a 10 mM $KMnO_4$ and 0.25 M H_2SO_4 solution. Three hundred milligrams of HS was oxidized for 1 h at 45 °C under stirring and N_2 atmosphere. Then, the resulting oxidized derivative was abundantly washed with deionized water until it reached a neutral pH and was freeze-dried.

Basic Oxidation with $KMnO_4$ (D2). Oxidation was carried out in 20 mL of a 10 mM $KMnO_4$ and 0.5 M KOH solution (*8*). Three hundred milligrams of HS was oxidized for 1 h at 45 °C under stirring and N_2 atmosphere. The resulting oxidized derivative was then dialyzed (3.5 kDa MW cutoff) against deionized water and freeze-dried.

Reduction with Sodium Borohydride (D3). The reaction was applied to 300 mg of HS using 400 mg of $NaBH_4$ dissolved in 50 mL of a 0.1 M NaOH solution (*10*). The reaction was allowed to proceed for 2 h under N_2 atmosphere. Subsequently, the solution containing the dissolved products was adjusted to pH 6.5 with 6 M HCl, dialyzed (3.5 kDa MW cutoff) against deionized water, and freeze-dried.

Alkaline Methanolic Hydrolysis (D4). The HS (300 mg) were placed in a three-neck round flask and hydrolyzed for 1 h under reflux at 75 °C with 20 mL of a 1 M KOH−CH_3OH solution under inert N_2 atmosphere (*11*). After recovery of the supernatant by centrifugation (15 min, 5000*g*) and filtration, the residue was again refluxed twice with 20 mL of CH_3OH for 30 min. The combined methanolic extracts were concentrated by rotoevaporation, acidified to pH 5 with 3 M HCl solution, and transferred into a separation funnel with 30 mL of deionized water. The released organic compounds were finally extracted with 30 mL of chloroform. The organic phase was concentrated, dehydrated with anhydrous Na_2SO_4, and evaporated at reduced pressure for further analysis. The hydrolyzed derivative was abundantly washed with deionized water and freeze-dried.

Acid Hydrolysis with H_2SO_4 (D5). The HS (300 mg) were hydrolyzed under reflux at 60 °C for 2 h with 25 mL of a 2 M H_2SO_4 solution (*12*). The suspension was filtered, and the hydrolyzed derivative was abundantly washed with deionized water and freeze-dried.

Acid Hydrolysis by Dioxane in 2 M HCl (D6). The HS (300 mg) were submitted to acidolysis with 20 mL of a dioxane solution containing 2 M HCl for 30 min under reflux at 60 °C and N_2 atmosphere (*13*). After recovery of supernatant by centrifugation (30 min, 6500*g*), the residue was washed three times with 10 mL of dioxane. The hydrolyzed derivative was washed abundantly with water and freeze-dried.

Extraction of Free Lipids (D7). Free and unbound alkyl components were extracted by shaking HS (300 mg) for 2 h at room temperature with a 15 mL solution of dichloromethane/methanol (2:1, v/v) (*11*). This extraction was repeated once more. The extracts were separated from residue by centrifugation (15 mim, 5000*g*) in Teflon tubes, and the supernatants were combined and dried by rotoevaporation supplemented with a minimum amount of dichloromethane/methanol for further analysis. The resulting humic derivative was freeze-dried.

Methylation (D8). Methylation was obtained by reaction with methyl iodide through a phase-transfer catalysis (*14*). The humic sample (300 mg) was suspended in 15 mL of tetrabutylammonium bromide ([$(CH_3$-$(CH_2)_3]_4$NBr) 20% in 1 M KOH. Twenty milliliters of tetrahydrofuran (THF) was then added to the suspension and stirred for 2 h at room temperature to ensure complete neutralization of acid protons and, hence, dissolution of HS in the alkaline [$(CH_3(CH_2)_3]_4$NBr. The methyl iodide alkyl halide was then added to the solution in approximately 5% molar excess (0.4 mL) relative to the molar content of acidic protons in HS. The reaction mixture was stirred overnight and then treated with 1 M HCl to adjust the pH to 7. The alkylating agent and THF were removed under reduced pressure at 50−70 °C, giving a solid residue. Residual CH_3-$(CH_2)_3]_4$NBr salts were removed from the reaction product by first washing the derivative with hot (60 °C) deionized water (50 mL) and, then, dialyzing it (3.5 kDa MW cutoff) against deionized water followed by freeze-drying.

Characterization of Humic Derivatives. *Elemental Composition.* The CHN elemental composition of HS and their reaction products was evaluated using a model 14800 CHN Perkin-Elmer autoanalyzer. The oxygen content was obtained by difference and the ash content by incinerating in a muffle furnace 50 mg of each sample at 700 °C for 8 h.

Analytical HPSEC. A solution of a phosphate buffer at pH 7 added with 0.3 g/L NaN_3 (bacteriostatic agent) was used to both dissolve and elute each humic derivative by analytical HPSEC. Samples (0.02 g/L) were filtered through glass microfiber filters before each analytical run. The analytical HPSEC system consisted of a Polysep P-300 column (250 mm × 7.8 mm i.d.) from Phenomenex (thermostated at 25 °C) and a Perkin-Elmer LC200 pump connected to two detectors in series: a Gilson 118 UV−vis detector set at 280 nm and a refractive index (RI) detector (Fisons Instruments, San Carlos, CA). To test column reproducibility, chromatograms of all size fractions were repeated either two or three times and relative standard deviation (RSD) of peak areas never exceeded 3%.

Solid-State NMR Spectroscopy (^{13}C CPMAS-NMR). Cross-polarization magic angle spinning (CPMAS) ^{13}C NMR spectra were acquired with a Bruker AVANCE 300 NMR spectrometer, equipped with a 4 mm wide-bore MAS probe, operating at a ^{13}C resonating frequency of 75.475 MHz. Samples (100−200 mg) were packed in 4 mm zirconia rotors with Kel-F caps and were spun at 13 ± 1 kHz. A ^{1}H ramp sequence was used during a contact time of 1 ms to account for possible inhomogeneity of the Hartmann−Hahn condition. Two thousand scans with 3782 data points were collected over an acquisition time of 25 ms and a recycle delay of 2.0 s. Bruker Topspin 1.3 software was used to collect and elaborate the spectra. All of the free induction decays (FID) were transformed by applying a 4K zero filling and a line broadening of 75 Hz. Spectra were integrated in the chemical shift (ppm) resonance intervals: 187−162 (carbonyls of ketones, quinines, aldehydes, and carboxyls), 162−112 (aromatic and olefinic carbons), 112−93 (anomeric carbons), 93−46 (C−O systems, such as alcohols and ethers, C−N groups, and complex aliphatic carbons), and 46−0 ppm (sp^3 carbon, mainly methylene and methyl). The relative areas of alkyl (46−0 ppm) and aromatic (162−112 ppm) components were summed to represent the proportion of hydrophobic carbons in humic samples (hydrophobic carbon, HB). Similarly, the summation of relative areas in intervals related to polar groups (187−162, 112−46) indicated the proportion of hydrophilic carbon (HI). The hydrophobic index (HB/HI) was then calculated.

Diffusion-Ordered NMR Spectroscopy (DOSY-NMR). Solution-state DOSY NMR spectra were obtained on a Bruker AVANCE 400 MHz instrument operating at a proton frequency of 400.13 MHz, equipped with a 5 mm Bruker inverse broadband probe. All spectra were elaborated by Bruker Topspin 1.3 (Bruker Biospin). Five milligrams of each freeze-dried HA was dissolved in 0.75 mL of deuterated water (D_2O) and transferred to 5 mm NMR quartz tubes fitted with Doty susceptibility plugs. ^{1}H NMR spectra were referenced to the chemical shift of solvent, resonating at 4.8 ppm, and ^{1}H 90° pulse was calibrated using HOD signal. 2D-DOSY diffusion-ordered spectra were obtained using a stimulated echo pulse sequence with bipolar gradients (STEBPGP) provided by a watergate 3−9−19 pulse train with gradients for presaturation of water signal. Scans (320) were collected using 2.5 ms sine-shaped pulses (5 ms bipolar pulse pair) ranging from 0.674 to 32.030 G/cm in 32 increments, with a diffusion time of 100−160 ms and 8K time domain data points. Apodization was made by multiplying data with a line broadening of 1.0 Hz, spike

suppression factor of 1.0, maximum interactions number set to 100, noise sensitivity factor of 2, and number of components set to 1. A mono-exponential decay without entropy minimization was applied during data processing. Diffusion coefficients of seven standard compounds of known molecular weight were measured to express diffusion as a function of molecular weight, from which diffusion data were approximated to molecular sizes. The selected standards methanol (32.0 Da), catechol (110.1 Da), caffeic acid (180.2 Da), catechin (290.0 Da), bromocresol green (698.0 Da), and two polystyrene sulfonates having 1100 and 6780 Da were dissolved and acquired in the same way as HS samples described above. Diffusion coefficients were elaborated using Bruker Topspin 1.3 software.

Plant Assays. *Arabidopsis*. Seeds of *A. thaliana* ecotype Columbia 4 were surface sterilized with 95% (v/v) ethanol for 5 min and with 0.5% (w/v) NaClO for 7 min. After five rinsings with distilled water, seeds were germinated and grown in a mini-hydroponic system (*15*). *Arabidopsis* were placed in a plant growth cabinet with a photoperiod of 16 h of light and 8 h of darkness, a light intensity of 90 μmol/m^2/s, and temperatures of 22 °C (night) and 24 °C (day). After 5 days in the cabinet, the five best plants were left in each plate and the germinating papers were rinsed four times with 1 mL of solutions containing HS. A minimum of distilled water was left in each ice tray cell to irrigate the plates by capillarity. After 3 days of treatment, the germinating papers were rinsed four times with 1 mL of a modified Hoagland solution with 1 mmol/L of N, as ammonium nitrate (*16*). This low N level was used to avoid root branching stimulation by nitrate. Three days later, this rinsing with nutrient solution was repeated. After 2 weeks of growth, the black covers and the germinating papers were taken off the plates; the roots, kept between the two other layers, were stained with toluidine blue (0.05%), and the images were digitalized by scanner (300 dpi) for root analysis by Delta-t scan software (Delta T Devices Ltd., Cambridge, U.K.). Two plants in the central position of the plates were chosen for evaluation of the number of lateral roots, length of the principal root, and density and length of lateral roots with four replicates.

Maize. Maize seeds (var. UENF 506) provided by UENF Plant Science Department were surface sterilized by soaking in 0.5% NaClO for 30 min, followed by rinsing and then soaking in water for 6 h. The seeds were then sown on wet filter paper and germinated in the dark at 28 °C. Four-day-old maize seedlings with roots of approximately 0.5 cm in length were transferred into a solution containing 2 mM $CaCl_2$ and either 0 or 20 mg of C dry wt/L of each HS extract with 10 replicates. A minimal medium (2 mM $CaCl_2$) was used. Maize seedlings were placed in a plant growth cabinet with a photoperiod of 10 h of light and 14 h of darkness, a light intensity of 120 μmol/m^2/s, and temperatures of 25 °C (night) and 28 °C (day). Roots were collected on the seventh day and scanned at 300 dpi to estimate their length and area using image analysis software Delta-T Scan (*17*). Additional samples of root seedlings were collected for further experiments.

Tomato. Tomato seeds (*S. lycopersicum* cv. Debora) were sterilized with commercial solution of 30% NaClO for 15 min, under agitation. Those seeds were washed with sterile water and sowed in boxes (11 × 11 × 4 cm) for germination. The boxes were conditioned in a growth chamber under the following conditions: 25 °C and 12 h photoperiod. After germination (4−5 days), the seedlings were treated with increasing concentrations (0, 0.1, 1.0, 3.0, 5.0, and 10.0 mM of C) of SH and their chemical derivatives with eight replicates for each treatment. Tomato seedlings were cultivated at the same growth conditions described above for maize. After regression analysis, a new experiment was carried out using the best concentration of each chemical derivative. The plants grew in the treatments for 5 days, and then they were evaluated for the number of emerged lateral roots, the length of the lateral roots, and the length of the principal roots.

Biochemical Assays. Plasma membrane (PM) vesicles were isolated from maize roots grown with and without 20 mg of C/L of bulk HS and each chemical derivative using the differential centrifugation method (*18*). The vesicles were either used immediately or frozen under liquid N_2 and stored at −70 °C until use. Protein concentrations were determined according to the Lowry method. ATPase activity in PM vesicles was determined by measuring colorimetrically the release of inorganic phosphorus (P_i). Between 80 and 95% of the PM vesicles ATPase activity measured at pH 6.5 was inhibited by vanadate (0.1 mmol/L), a very effective inhibitor of the P-type H^+-ATPases. In all experiments, ATPase activity was measured at 30 °C, with and without vanadate, and the difference between these two activities was attributed to the plasma membrane H^+-ATPase.

Micro-Tom DR5-GUS Labeling Assay. Four-day-old DR5::GUS transgenic Micro-Tom tomato plants were treated with HS and their chemical derivatives for easier detection of auxin-like activity. The tomato seedlings were treated for 4 days with 4.5 mM C of HS and their derivatives after the appropriate concentration for each derivative had been determined, as described above, or with 2 mM $CaCl_2$ as a control. Histochemical GUS staining was performed as described previously (*19*) with minor modifications of incubating root segments for 1 day in a dark room with the GUS solution at 37 °C. The results were observed by visualization in light microscope of the diffuse blue product of the enzymatic reaction in root segments. The seeds were kindly provided by Dr. José Luiz Garcia-Martinez from the Universidad Politécnica de Valencia, Spain.

Statistical Analysis. The biological activities of original HS and reaction products were subjected to preliminary regression analysis to identify the most appropriate concentration to enhance lateral root emergence. Then new experiments with original HS and reaction products were conducted at the selected concentration, the variance was analyzed (ANOVA), and the means were compared (DMS $p < 0.05$). After the preliminary screening, the descriptors with a high degree of autocorrelation were eliminated, and a systematic search of multilinear regression with one, two, or three members was conducted using BuildQSAR software to identify the chemical properties most closely related to bioactivity.

RESULTS

Elemental Characterization. The elemental composition of the bulk HS and their derivatives is shown in **Table 1**. Methanolic alkaline hydrolysis (D4) produced the greatest decrease in C content with respect to unmodified HS, whereas other chemical modifications invariably increased C content in humic derivatives. The N content in the derivatives was mostly reduced in methanolic alkaline hydrolysis (D4), remained similar to the control after acidic dioxane hydrolysis (D6) and methylation reaction (D7), and was considerably enhanced after all other treatments. Despite C and N content variations, the C/N ratio showed no changes, except for the acidic dioxane hydrolysis (D6), which accounted for a large C increase (**Table 1**). The H content was diminished somewhat by alkaline methanolic hydrolysis (D4), whereas there was little change for other reactions.

CP/MAS ^{13}C NMR. The carbon distribution in the original HS and derivatives was revealed by CPMAS ^{13}C NMR spectra. The original HS spectrum shows signals in the alkyl-C (0−46 ppm) and C−O/C-N (46−112 ppm) regions corresponding, respectively, to methylene and terminal methyl groups of waxes and polyesters, and methoxy groups of guaiacyl, the major lignin compounds in grass, as well as C2, C3, and C5 and anomeric-C (103 ppm) of cellulose and hemicellulose units (*20*). The aromatic-C region is characterized by a broadband centered at 136 ppm of overlapping resonances of unsubstituted and substituted benzene rings and by a smaller signal on 151 ppm assigned to phenolic C. A prominent and sharp signal of quaternary carbons at 173 ppm is currently assigned to carboxyl groups, esters, and amides (*21*). Compared to the original HS, spectra of humic derivatives showed variable changes mainly in the relative intensities of such spectroscopic signals.

Table 1 reports percent carbon distribution from integration of spectra of humic materials after various chemical reactions. The carboxylic content was only slightly affected by the reactions, except for a decrease after the H_2SO_4 hydrolysis (D5). Aromatic and phenolic C increased substantially after acidic reactions (D1, D5, and D6) and slightly after extraction of free lipids (D7), but did not change after other reactions. The C−O/C−N signals were reduced mainly in HS submitted to $KMnO_4$ oxidations and H_2SO_4 hydrolysis (D5). Alkyl-C signals increased with $KMnO_4$

Table 1. Elemental Content, H/C and C/N of Original Bulk HS and Reaction Products, and Distribution of C Intensity in Different Regions of ^{13}C NMR Spectra of Bulk HS and Their Reaction Derivatives

	elemental composition (%)					chemical shift (CP-MAS ^{13}C NMR)					
sample[a]	C	H	N	H/C	C/N	0−40 ppm	40−110 ppm	110−160 ppm	160−200 ppm	HBHI[b]	aromaticity[c]
bulk HS	25.24	2.38	2.74	1.30	12.37	23.20	42.90	23.90	10.00	0.89	4.18
D1	28.14	2.80	4.32	1.84	11.71	25.40	38.70	26.20	9.80	1.06	3.82
D2	31.25	3.02	4.07	1.56	12.09	24.70	39.90	25.10	10.20	0.99	3.98
D3	25.00	2.24	3.69	1.77	13.01	22.00	43.90	24.20	9.90	0.86	4.13
D4	21.64	1.99	2.04	1.13	12.69	21.20	42.40	25.80	10.60	0.89	3.87
D5	31.60	2.94	3.37	1.28	12.54	25.70	35.10	30.70	8.50	1.29	3.25
D6	47.84	3.08	2.71	0.68	18.12	20.80	42.70	27.30	9.30	0.93	3.66
D7	27.60	2.38	2.69	1.17	13.53	20.30	43.30	25.60	10.80	0.85	3.90
D8	33.23	2.98	4.40	1.59	13.02	25.00	41.20	23.90	9.90	0.96	4.18

[a] D1, acidic oxidation with $KMnO_4$; D2, basic oxidation with $KMnO_4$; D3, reduction with sodium borohydride; D4, alkaline methanolic hydrolysis; D5, acid hydrolysis with H_2SO_4; D6, acid hydrolysis by dioxane in 2 M HCl; D7, extraction of free lipids; D8, methylation. [b] Hydrophobic carbon/hydrophilic carbon = [(0−40) + (110−160)]/[(40−110) + (160−200)]. [c] (110−160)/(0−200).

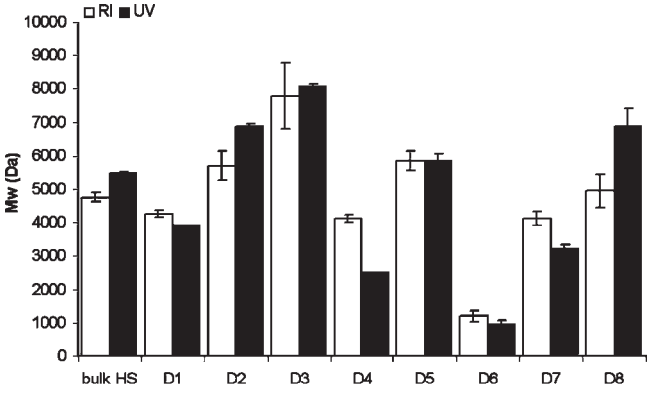

Figure 1. M_{wa} of bulk HS and their reaction derivatives as determined by both UV and RI detectors.

oxidations, H_2SO_4 hydrolysis, and methylation, whereas they were decreased by sodium borohydride reduction (D3), both methanolic alkaline (D4) and dioxane acid hydrolysis (D6), and extraction of unbound lipids (D7).

These structural changes in humic derivatives were reflected in the hydrophobic index (HB/HI). Reactions of H_2SO_4 hydrolysis (D5), oxidations (D1 and D2), and methylation (D8) increased the hydrophobic character of humic derivatives, whereas extraction of free lipids (D7) decreased their hydrophobicity. Despite the significant changes on elemental composition and NMR profile, the rest of the modified HS did not show substantial HB variations (**Table 1**). Most chemical modifications somewhat increased the intensity of aromatic and phenolic C in humic derivatives, with the exception of methylation (**Table 1**).

HPSEC. The HPSEC chromatograms of HS and their chemical derivatives were elaborated to obtain their apparent weight-average molecular weight (M_{wa}) (**Figure 1**). Measurements of M_{wa} based on UV−vis detection had a good reproducibility, whereas those measured by the RI detector were less precise. However, both detectors indicated that M_{wa} values decreased significantly when HS were submitted to acidic permanganate oxidation (D1), methanolic alkaline hydrolysis (D4), dioxane acid hydrolysis (D6), and extraction of free lipids (D7). On the other hand, alkaline permanganate oxidation, reduction with sodium borohydride, and H_2SO_4 hydrolysis increased the M_{wa} of HS. The methylation of HS (D8) showed very closed and larger M_{wa} with respect to control, respectively, when RI and UV−vis detectors were used. These phenomena were previously observed by Piccolo et al. (*28*) and attributed to conjugation of chromophorus components on humic solution that increase light absorption.

DOSY-NMR. Compared to the original HS, the derivative resulting from H_2SO_4 hydrolysis (D5) showed proton ("aromatic") signals in the 9.0−5.0 ppm range belonging to larger molecular size components, whereas those from $KMnO_4$ oxidation (D1), sodium borohydride reduction (D3), and acid hydrolysis in dioxane (D6) showed humic constituents of lower molecular size (**Figure 2**). The components in the C−O/C−N (polysaccharides) 4.4−2.9 ppm interval were mainly of lower molecular size than in control HS, with D6 showing the lowest values, except for D2 ($KMnO_4$ basic oxidation) and D7 (free-lipids removal) materials, which did not change significantly from control. Concomitantly, the 2.9−0.0 ppm range (aliphatic) indicates a molecular size increase of alkyl components for the H_2SO_4 hydrolysis (D5), whereas the rest of the HS derivatives resulted in lower molecular size than for the corresponding interval of the original control HS, with the exception of methanolic alkaline hydrolysis (D4), that was not significantly different from control. Methylation reaction (D8) promotes decrease in molecular size of all organic components (aromatic, aliphatic, and carbohydrates) with respect to control (**Figure 2**).

Effects of HS and Their Derivatives on Root Growth. The most appropriate concentrations of HS to induce lateral root emergence were 3.87, 2.05, and 4.54 mM C for *Arabidopsis*, maize, and tomato, respectively. The methylated derivative (D8) gave the lowest optimal concentration for induction of lateral root emergence for all plant species, whereas this optimal dose was provided by potassium permanganate oxidation (D1) for maize and tomato plants. The inflection point of quadractic equations (optimal concentration) was used to compare the original HS with their derivatives in an independent experiment. Emergence of lateral roots increased from 1.37- to 3.10-fold in maize (**Figure 3B**) and from 1.5- to 3.75-fold in *Arabidopsis* (**Figure 3A**), but the most dramatic effect was observed for tomato, in which it increased the emergence of lateral roots up to 10-fold (**Figure 3C**). Whereas all humic materials induced lateral root emergence, larger effects were produced by the acidic $KMnO_4$ oxidation (D1), methanolic alkaline hydrolysis (D4), acid hydrolysis in dioxane and H_2SO_4 (D5 and D6, respectively), and methylation (D8). The length of lateral roots was also modified by both the original control HS and their derivatives (**Figure 3 D−F**).

Effects of HS and Their Derivatives on PM H^+-ATPase Activity. Treatment with D1, D2, D5, and D8 promoted stimulations of the PM H^+-ATPase activity from 120 to 208% (**Figure 4**). The same derivatives promoted some of the largest increases in the number of emerged lateral roots (**Figure 3**). A significant correlation between the H^+ pump activation and the hydrophobic index of humic derivative was observed (**Table 2**).

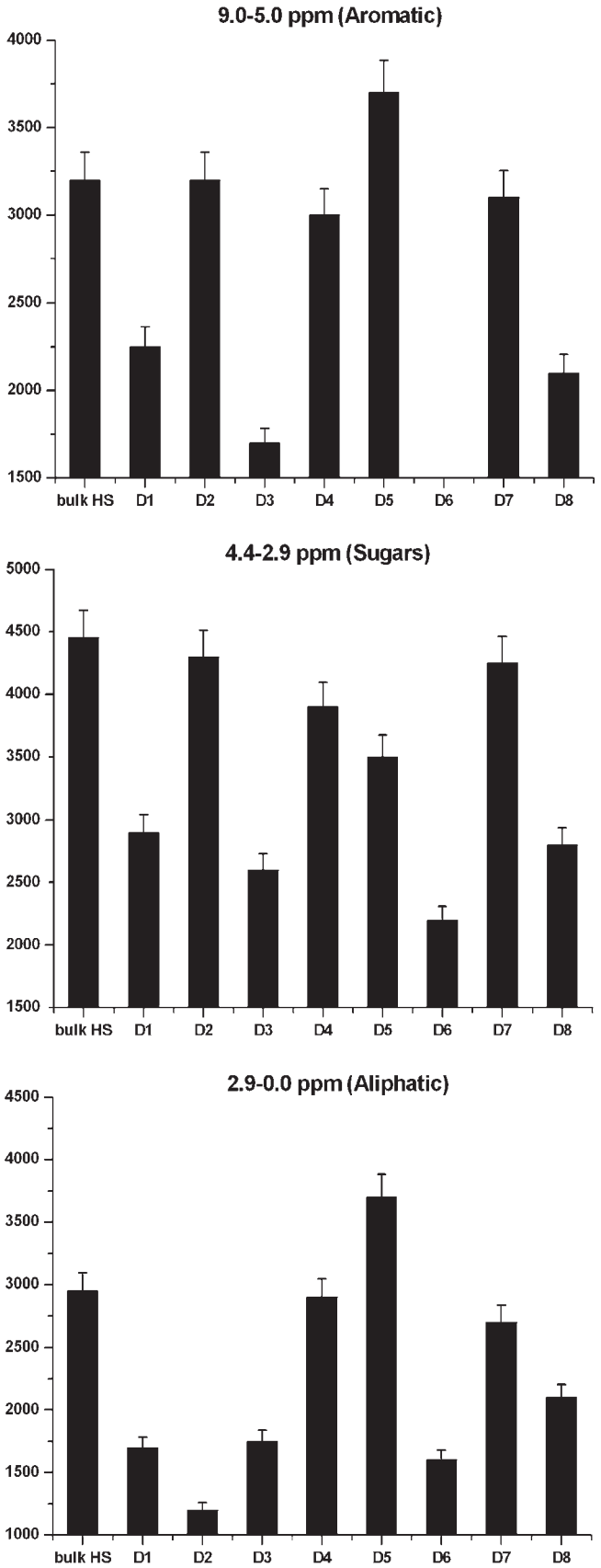

Figure 2. Molecular size (M_w) of bulk HS and their reaction derivatives as obtained from diffusion coefficients in DOSY ^{1}H NMR spectra and calibration curve of standards of known molecular weight.

Micro-Tom DR5::GUS Labeling Assay. The effect of HS and their chemical derivatives on induction of the auxin responsive synthetic reporter DR5::GUS of tomato (*S. lycopersicum* cv. Micro-Tom) can be observed in **Figure 5**. DR5::GUS has been used as a tool to visualize auxin responses in tissues and mark auxin signaling in roots. All treatments with HS or their derivatives extended the expression of DR5::GUS beyond that observed in the control treated with water (**Figure 5**). The presence of auxin activity in sites other than that commonly attributed to endogenous auxin accumulation indicates an auxin-like activity for HS and their derivatives.

DISCUSSION

Root development is a key requirement for plants to adapt and survive in adverse conditions and, therefore, lateral root number and placement are dramatically influenced by external factors. Although chemical reactions change the structure of HS derivatives, including carbon distribution, M_{wa}, and diffusion coefficients in water, their root growth promoter bioactivity was retained. No general relationship was found between the changes in apparent molecular size of HS, as measured by either HPSEC or DOSY-NMR, and the humic-induced root growth. These observations are in agreement with previous work that found induction of root growth in all humic acid size fractions obtained by HPSEC (*2*). Nevertheless, we observed that humic residues resulting from $KMnO_4$ acidic oxidation (D1) and methyl alkylation (D8), which most stimulated root growth and induced PM H^+-ATPase activity (**Figures 3** and **4**), were among the reaction products most significantly reduced in size for all three components measured by DOSY-NMR (**Figure 2**). Moreover, the humic product from dioxane acid hydrolysis (D6), which showed a very significant effect on the principal root length for all three plants (**Figure 3**), but failed to increase PM H^+-ATPase activity (**Figure 4**), revealed the lowest molecular size by both HPSEC (**Figure 1**) and DOSY-NMR (**Figure 2**). The reduction in size of these humic derivatives was accompanied by an increase in hydrophobicity index, as compared to the original HS (**Table 1**).

On the other hand, the humic material from H_2SO_4 hydrolysis (D5), which showed a still significant bioactivity (number of lateral root, length of primordial root, root density, and PM H^+-ATPase activity) for all three plants, had a molecular size greater that bulk HS base on both HPSEC and DOSY-NMR and the largest hydrophobicity of all humic samples. Furthermore, the derivative resulting from the $KMnO_4$ basic oxidation (D2) showed a significant stimulation of lateral root number (**Figure 3**) and density for *Arabidopsis* and tomato and the greatest PM H^+-ATPase activity on maize (**Figure 4**). Although this material did not differ in the diffusion of aromatic and polysaccharides from that of original HS, it did show the lowest alkyl component size on DOSY-^{1}H NMR (**Figure 2**) and still a substantially larger hydrophobicity than the control HS (**Table 1**). Finally, the derivatives less generally bioactive toward the tested plants were those obtained from reduction (D3), methanolic alkaline hydrolysis (D4), and lipid removal reactions (D7). Whereas D4 and D7 did not show a DOSY-NMR molecular size significantly different from the original HS, D3 had one of the lowest molecular sizes by diffusion measurements. It is interesting that D3 still revealed a capacity to increase PM H^+-ATPase activity (**Figure 4**). However, these three latter derivatives were the least hydrophobic materials among all humic samples.

These findings seem to indicate that, although the relationship between bioactivity and molecular size was not significant, other chemical features such as hydrophobic index appear to play an important role in the bioactivity of the modified humic matter from vermicompost. In a previous work, a correlation was

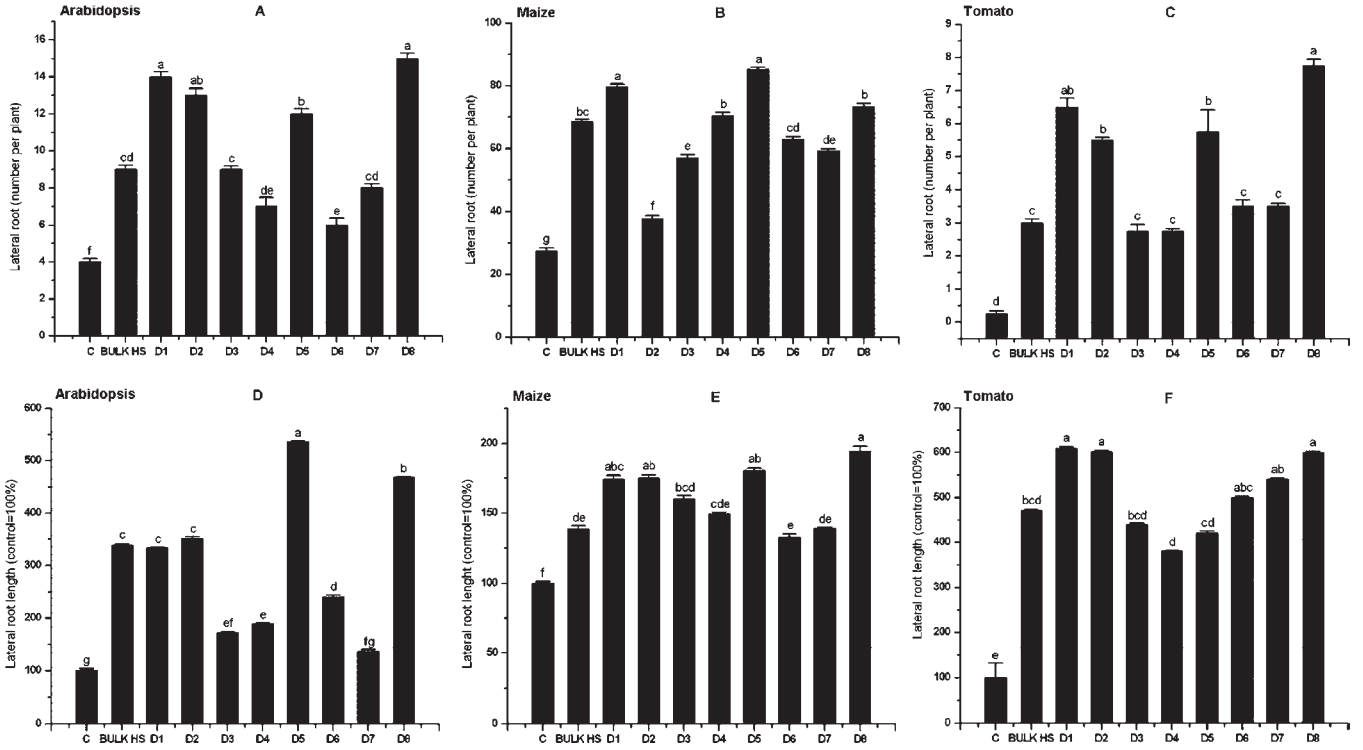

Figure 3. Number of emerged lateral roots (**A**−**C**) and length of lateral root (**D**−**F**) for *Arabidopsis*, maize, and tomato, respectively, treated with the best dose (mM C) solution of bulk humic substances (HS) and their reaction derivatives. Different lower case letters correspond to significant statistical differences between means with DMS test ($p < 0.05$).

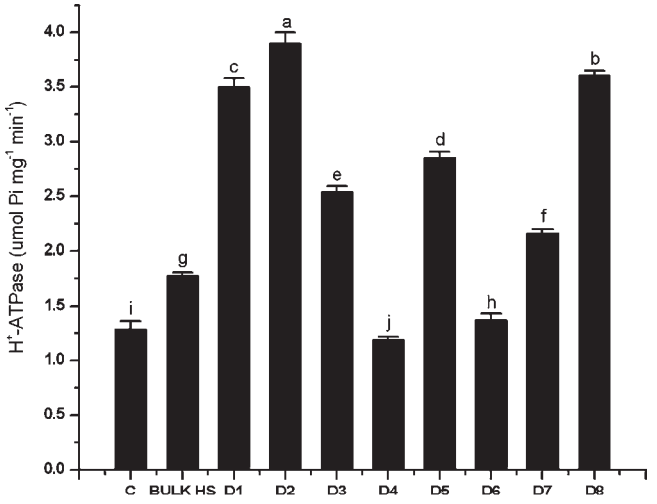

Figure 4. Plasma membrane H^+-ATPase activity from root vesicles isolated from maize seedlings treated with the best dose (mM C) solution of bulk HS and their reaction derivatives.

Table 2. Variable Selection to Linear Regression To Describe H^+-ATPase Activities from Maize Root Vesicles by Systematic Use of One Variable after Pearson Correlation Matrix[a]

C-AR	C-ALk	HBHI	M_wRI	%C	%N	*R*	SD	*F*	*p* <
●						0.673	139.676	3.952	0.1065
	●					0.478	146.127	1.526	0.4016
		●				**0.845**	**85.545**	**12.462**	**0.0167***
			●			0.320	153.971	0.563	0.4991
				●		0.663	128.102	3.195	0.1754
					●	0.532	134.116	2.273	0.1095

[a] C-AR, aromatic C (NMR ^{13}C, 165−130 ppm); C-Alk, alkyl C (NMR ^{13}C, 0−48 ppm); HBHI, hydrophobic index (0−48 + 165−130 ppp/50−110 + 165−200 ppm); M_wRI, molecular size distribution by HPSEC using RI as detector; %C, C content; %N, N content; *R*, correlation coefficient; SD, standard deviation of regression; *F* = Fisher test; *P*, probability of *F* test significance. *, H^+-ATPase activity = +1375.93 HBHI − 1373.31.

observed between hydrophobicity and biological activity from different HA isolated from different soils (*3*, *4*).

The root acidification mediated by plasma membrane H^+-ATPase is important for the regulation of cytoplasmic pH and the activation of cell wall-losing enzymes and proteins through acidification of apoplast (*22*). This effect is closely related to the auxin-induced cell growth as proposed by the acid growth theory in ref *5*. It has been earlier postulated that some HS may include compounds similar to indolacetic acid in their structure, and the capacity of HS to promote root growth was attributed to these compounds (*23*, *24*). In fact, humic complex structures can be disrupted by simple organic acids exuded by plant roots and microbes (*25*, *26*), and small auxin-like molecules may then be released and act on the cell receptors in plasma membrane (*27*). Early evidence for an auxin activity of HS was provided by their ability to induce the same molecular target of auxins, such as H^+-ATPase (*18*, *24*), and by the finding that different humic acids were unable to induce lateral roots in a Micro-Tom tomato mutant insensitive to auxin (*15*). Here, the induction of the auxin responsive synthetic reporter DR5::GUS in transgenic Micro-Tom tomato plants by HS (**Figure 5**) is clear evidence of the auxin activity of such substances, as proposed previously (*1*, *15*, *18*, *24*). Because all humic derivatives were also able to induce this specific auxin response element, it is likely that the auxin activity of humic substances resides somewhere in their common structure. Such findings may provide for further research aiming at unraveling the molecular identity of the auxin-like substance(s) present in HS (*15*, *18*, *24*).

On the basis of a number of chromatographic and NMR results, HS have been described, instead of being cross-linked macropolymers, as a supramolecular mixture of partially

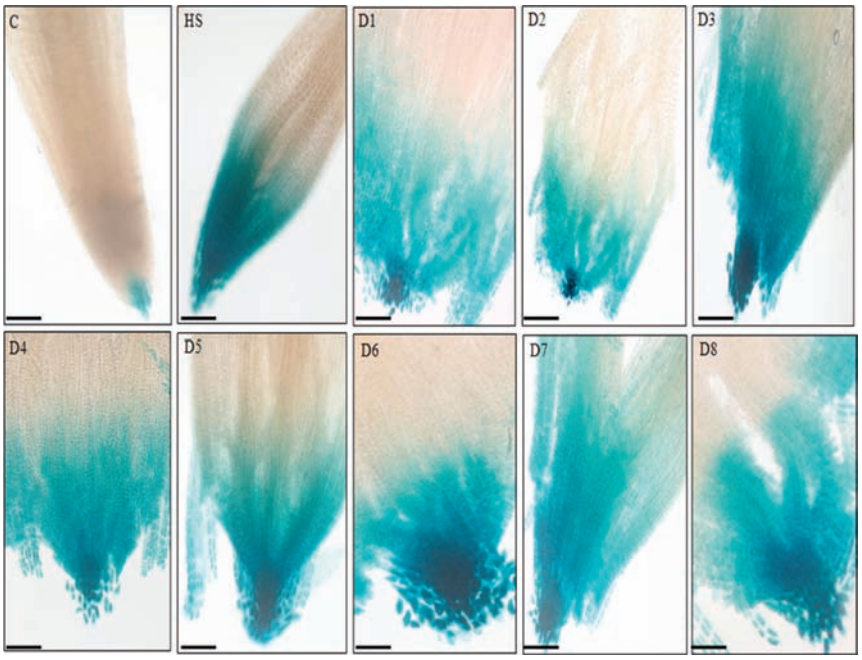

Figure 5. Visualization of GUS activity in root of DR5::GUS transgenic tomato. Seedlings were grown for 4 days in 2 mM $CaCl_2$ medium and then incubated for 4 days in water (C), 4.5 mM C of humic substance (HS), or its derivatives (D1−D8). Scale bar is 100 μm.

transformed biomolecules of relatively low molecular weight held together by weak associations, mainly represented by hydrophobic interactions, in only apparently large molecular sizes (*28*). This concept of supramolecular aggregation of relatively small heterogeneous humic molecules was supported experimentally (*29*, *30*). A consequence of this concept is that the bioactivity of humic matter is to be more related to how humic molecules are mutually associated and their conformational size and strength than to specific structural diversities (*3*).

Here, we found that chemical modifications of a humic structure affect its root growth in three plant species. The chemical modifications varied the composition, hydrophobic index, and component molecular sizes in humic superstructures, and this was reflected in their capacity to interact with plant cells. Although no relationship was shown between molecular size and humic bioactivity, we found here that the hydrophobic index seems to be a suitable criterion to evaluate humic effects on root growth. This suggests that this derivative has the least stable conformation and the largest probability to release auxin-like molecules to maize cell receptors. It thus appears that HS bioactivity on plants depends on a sufficient hydrophobicity index to allow interactions with plant root cells, but the hydrophobic domains should concomitantly possess a conformation sufficiently labile to release, possibly by the action of acidic root exudates, auxin-like molecules that exert a biological stimulation (**Figure 5**).

Supporting Information Available: CP/MAS ^{13}C NMR spectra, regression analysis of root growth, and all best doses of HS and its derivatives used in *Arabidopsis*, maize, and tomato assays. This material is available free of charge via the Internet at http://pubs.acs.org.

LITERATURE CITED

(1) Trevisan, S.; Pizzeghello, D.; Ruperti, B.; Francioso, O.; Sassi, A.; Palme, K.; Quaggiotti, S.; Nardi, S. Humic substances induce lateral root formation and expression of the early auxin-responsive IAA19 gene and DR5 synthetic element in *Arabidopsis*. *Plant Biol*. **2010**, doi: 10.1111/j.1438-8677.2009.00248.x.

(2) Canellas, L. P.; Spaccini, R.; Piccolo, A.; Dobbss, L. B.; Okorokova-Façanha, A. L.; Santos, G. A.; Olivares, F. L.; Façanha, A. R. Relationships between chemical characteristics and root growth promotion of humic acids isolated from Brazilian oxisols. *Soil Sci*. **2009**, *174*, 611–620.

(3) Canellas, L. P.; Zandonadi, D. B.; Busato, J. G.; Baldotto, M. A.; Simões, M. L.; Martin-Neto, L.; Façanha, A. R.; Spaccini, R.; Piccolo, A. Bioactivity and chemical characteristics of humic acids from tropical soils sequence. *Soil Sci*. **2008**, *173*, 624–637.

(4) Canellas, L. P.; Piccolo, A.; Dobbss, L. B.; Olivares, F. L.; Spaccini, R.; Zandonadi, D. B.; Façanha, A. R. Chemical composition and bioactivity properties of size-fractions separated from a vermicompost humic acids. *Chemosphere* **2010**, *78*, 457–466.

(5) Rayle, D. L.; Cleland, R. E. The acid growth theory of auxin-induced cell elongation is alive and well. *Plant Physiol*. **1992**, *99*, 1271–1274.

(6) Piccolo, A. Humus and soil conservation. In *Humic Substances in Terrestrial Ecosystems*; Piccolo, A., Ed.; Elsevier: Amsterdam, The Netherlands, 1996; pp 225−264.

(7) Greenland, D. J.; Hayes, M. H. B. *The Chemistry of Soil Constituents*; Wiley: Chichester, U.K., 1978.

(8) Schnitzer, M.; Desjardins, J. G. Alkaline permanganate oxidation of methylated and unmethylated fulvic acid. *Soil Sci. Soc. Am. Proc*. **1970**, *34*, 77–79.

(9) Hayes, M. H. B.; MacCarthy, P.; Malcolm, R. L.; Swift, R. S. In *Humic Substances II, In Search of Structure*; Hayes, M. H. B., MacCarthy, P., Malcolm, R. L., Swift, R. S., Eds.; Wiley: Chichester, U.K., 1989; pp 3−32.

(10) Thorn, K.; Pettigrew, P.; Goldenberg, W.; Weber, E. Covalent binding of aniline to humic substances. 2. ^{15}N NMR studies of nucleophilic addition reactions. *Environ. Sci. Technol*. **1996**, *30*, 2764–2775.

(11) Spaccini, R.; Piccolo, A. Molecular characterization of compost at increasing stages of maturity. 1. Chemical fractionation and infrared spectroscopy. *J. Agric. Food Chem*. **2007**, *55*, 2293–2302.

(12) Oades, J. M.; Kirkman, M. A.; Wagner, G. H. The use of gas−liquid chromatography for the determination of sugars extracted from soils by sulphuric acids. *Soil Sci. Soc. Am. Proc*. **1970**, *34*, 230–235.

(13) Fukushima, R. S.; Hatfield, R. D. Espectro de duas formas de lignina obtidos por ressonância magnética nuclear. *Pesq. Agropec. Bras*. **2003**, *38*, 505–511.

(14) Piccolo, A.; Conte, P.; Patti, A. F. O-Alkylation of a lignite humic acid by phase-transfer catalysis. *Anal. Bional. Chem*. **2006**, *384*, 994–1001.

(15) Dobbss, L. B.; Medici, L. O.; Peres, L. E.; Pino-Nunes, L. E.; Rumjanek, V. M.; Façanha, A. R.; Canellas, L. P. Changes in root development of Arabidopsis promoted by organic matter from oxisols. *Ann. Appl. Biol.* **2007**, *151*, 199–211.

(16) Medici, L. O.; Azevedo, R. A.; Smith, R. J.; Lea, P. J. The influence of nitrogen supply on antioxidant enzymes in plant roots. *Fundam. Plant Biol.* **2006**, *31*, 1–9.

(17) Bouma, T. J.; Nilsen, K. L.; Koutstaal, B. Sample preparation and scanning protocol for computerised analysis of root length and diameter. *Plant Soil* **2000**, *218*, 185–196.

(18) Canellas, L. P.; Façanha, A. O.; Olivares, F. L.; Façanha, A. R. Humic acids isolated from earthworm compost enhance root elongation, lateral root emergence, and plasma membrane H^+-ATPase activity in maize roots. *Plant Physiol.* **2002**, *130*, 1951–1957.

(19) Jefferson, R. A.; Kavanagh, T. A.; Bevan, M. W. GUS fusions: β-glucuronidase as a sensitive and versatile gene fusion marker in higher plants. *EMBO J.* **1987**, *6*, 3901–3907.

(20) Spaccini, R.; Piccolo, A. Spectroscopic characterization of a compost at different maturity stages. *Clean* **2008**, *36*, 152–157.

(21) Knicker, H.; Almendros, G.; Gonzalex-Vila, F. J.; Ludemann, H. D.; Martin, F. C-13 and N-15 NMR analysis of some fungal melanins in comparison with soil organic matter. *Org. Geochem.* **1995**, *23*, 1023–1028.

(22) Sze, H.; Li, X.; Palmgren, M. G. Energization of plant cell membranes by H^+-pumping ATPases: regulation and biosynthesis. *Plant Cell* **1999**, *11*, 677–689.

(23) Muscolo, A.; Cultrupi, S.; Nardi, S. IAA detection in humic substances. *Soil Biol. Biochem.* **1998**, *30*, 1199–1201.

(24) Zandonadi, D. B.; Canellas, L. P.; Façanha, A. R. Indolacetic and humic acids induce lateral root development through a concerted plasmalemma and tonoplast H^+ pumps activation. *Planta* **2007**, *225*, 1583–1595.

(25) Piccolo, A.; Conte, P.; Cozzolino, A. Effects of mineral and monocarboxylic acids on the molecular association of dissolved humic substances. *Eur. J. Soil Sci.* **1999**, *50*, 687–694.

(26) Piccolo, A.; Conte, P.; Trivellone, E.; Van Lagen, B.; Buurman, P. Reduced heterogeneity of a lignite humic acid by preparative HPSEC following interaction with an organic acid. Characterization of size-separates by PYR-GC-MS and ^{1}H-NMR spectroscopy. *Environ. Sci. Technol.* **2002**, *36*, 76–84.

(27) Canellas, L. P.; Teixeira Junior, L. R. L.; Dobbss, L. B.; Silva, C. A.; Medici, L. O.; Zandonadi, D. B.; Façanha, A. R. Humic acids crossinteractions with root and organic acids. *Ann. Appl. Biol.* **2008**, *153*, 157–166.

(28) Piccolo, A. The supramolecular structure of humic substances: a novel understanding of humus chemistry and implications in soil science. *Adv. Agron.* **2002**, *75*, 57–154.

(29) Simpson, A. J. Determining the molecular weight, aggregation, structures and interactions of natural organic matter using diffusion ordered spectroscopy. *Magn. Reson. Chem.* **2002**, *40*, 572–582.

(30) Smejkalova, D.; Piccolo, A. Aggregation and disaggregation of humic supramolecular assemblies by NMR diffusion ordered spectroscopy (DOSY-NMR). *Environ. Sci. Technol.* **2008**, *42*, 699–706.

Received for review December 11, 2009. Revised manuscript received February 10, 2010. Accepted February 11, 2010. L.P.C. gratefully acknowledges a fellowship from CAPES that sponsored a scientific visit to Italy. CNPq, FAPERJ, and IFS provided financial support for this research.